Smart Mater. Struct. **19** (2010) 115006 (13pp) doi:10.1088/0964-1726/19/11/115006

Soft capacitor fibers using conductive polymers for electronic textiles

Jian Feng Gu, Stephan Gorgutsa and Maksim Skorobogatiy

Génie Physique, École Polytechnique de Montréal, Montréal, H3C 3A7, Canada

E-mail: maksim.skorobogatiy@polymtl.ca

Received 10 April 2010, in final form 23 August 2010
Published 21 September 2010
Online at stacks.iop.org/SMS/19/115006

Abstract

A novel, highly flexible, conductive polymer-based fiber with high electric capacitance is reported. In its cross section the fiber features a periodic sequence of hundreds of conductive and isolating plastic layers positioned around metallic electrodes. The fiber is fabricated using the fiber drawing method, where a multi-material macroscopic preform is drawn into a sub-millimeter capacitor fiber in a single fabrication step. Several kilometers of fibers can be obtained from a single preform with fiber diameters ranging between 500 and 1000 μm. A typical measured capacitance of our fibers is 60–100 nF m^{-1} and it is independent of the fiber diameter. Analysis of the fiber frequency response shows that in its simplest interrogation mode the capacitor fiber has a transverse resistance of 5 kΩ m L^{-1}, which is inversely proportional to the fiber length L and is independent of the fiber diameter. Softness of the fiber materials, the absence of liquid electrolyte in the fiber structure, ease of scalability to large production volumes and high capacitance of our fibers make them interesting for various smart textile applications ranging from distributed sensing to energy storage.

(Some figures in this article are in colour only in the electronic version)

1. Introduction

Fueled by the rapid development of micro- and nanotechnologies, and driven by the need to increase the value of conventional textile products, fundamental and applied research into smart textiles (or high-tech textiles) has recently flourished. Generally speaking, textiles are defined as 'smart' if they can sense and respond to the environmental stimuli that can be of mechanical, thermal, chemical, electrical, magnetic, etc, nature. Some of the first uses of smart textiles were in military and medical applications. For example, with the support of the US Naval Department in 1996 Georgia Tech has developed a garment called Wearable Motherboard (with the commercial name of Smart shirt) [1, 2]. The Wearable Motherboard is a fabric featuring woven electric wires and/or optical fibers that serve as a flexible information bus. To integrate electronics directly into textiles leads to the so-called technique of 'wearable computing' or 'e-textiles' [3–5]. Another application of smart textiles is in harnessing (and recently in storage) of the energy of human motion or the energy of various ambient fields, such as electromagnetic fields. Electric energy generation from human motion, for example, has recently been demonstrated using piezoelectric fibers made of ceramic materials like PZT (lead zirconate titanate) as well as polymers such as PVDF (polyvinylidene fluoride) [6, 7]. Smart textiles can also find their use in heat-storage and thermo-regulated clothing [8, 9] and various wearable sensors including those for biomedical monitoring [10]. For example, conventional fabrics coated with a thin conducting polymer layer possess remarkable properties of strain and temperature sensing [11]. A multilayer structure consisting of two conductive fabrics separated by a meshed non-conductive one can be used as a pressure sensor [10]. Sensing garments for monitoring physiological and biomechanical signals of the human body have already been invented for healthcare [12] and sports training [13]. Other applications of smart textiles have been demonstrated from responsive seats in automobiles [14], where textiles can indicate the level of comfort of an individual passenger, to apparel with tunable or adjustable color and appearance in fashion and design [15]. With the constant improvement of the technology, there is no doubt that smart textiles will soon become an integral part of our daily life [16–18].

Most of the 'smart' functionalities in the early prototypes of smart apparel are enabled by integrating conventional rigid electric devices into a textile matrix, which did not provide

acceptable wearing comfort. This motivated recent efforts into the development of truly wearable smart textiles. Progress in this direction has already been made by using all-polymer materials and exploring special fabrication methods [12, 19]. The high flexibility and softness of the integrated devices not only improves the wearability of smart textiles but also ensures sensors have close contact with the body, which is important for biomedical and healthcare measurements. For example, a fully flexible piezoresistive sensor for capturing posture or detecting respiration has been fabricated by coating a thin layer of piezoresistive materials, such as polypyrrole (PPy) or a mixture of rubbers and carbons, on conventional fabrics [11]. Such sensors were then integrated into textiles by flat knitting technology, which makes the garment really wearable [12, 20]. Nevertheless, such sensors may suffer from strong variations in time of their resistance and high response time [19]. Advances in flexible energy storage materials also encourage their applications in wearable e-textiles. As reported in [21], a nanocomposite paper, engineered to function as both a lithium-ion battery and a supercapacitor, can provide a long and steady power output. A stretchable, porous and conductive textile has been manufactured by a simple 'dipping and drying' process using a single-walled carbon nanotube (SWNT) ink [22]. The loading of pseudocapacitor materials into this conductive textile can lead to a 24-fold increase of the areal capacitance of the device. A nitroxide radical functional polymer was photocrosslinked by Suga *et al* [23]. It can form a cathode-active thin film that leads to an organic-based paper battery. Recently a rechargeable textile battery was created by Bhattacharya *et al* [24]. It was fabricated on a textile substrate by applying a conductive polymeric coating directly over interwoven conductive yarns. Approaches to produce stretchable and foldable integrated circuits have also been reported. This includes integrating inorganic electronic materials with ultrathin plastic and elastomeric substrates [25] and printing highly viscous conductive ink onto nonwoven fabrics [26]. Ideally, if the electronic functionalities could be realized in a flexible fiber itself, such a fiber would provide a perfect building material for smart apparel as they could be naturally integrated into textiles during the weaving process. This would be a more suitable solution to the wearable smart textiles. Thus, a conductive fiber, prepared from ultra-high molecular weight polyaniline by continuous wet spinning techniques, was recently commercialized [27]. Shim *et al* demonstrated that commodity cotton threads can be transformed into smart electronic yarns and wearable fabrics for human biomonitoring using a polyelectrolyte-based coating with carbon nanotubes (CNTs) [28]. Besides fabric-based sensors, researchers have found approaches to make fiber-based or yarn-based piezoresistive sensors, including knitting conductive fibers with non-conductive base fibers [29] and wrapping piezoresistive carbon-coated fibers over a composite core yarn which was first integrated by the polyester fibers and elastic fibers [30]. In order to ensure a higher flexibility for piezoelectric sensors, cylindrical PVDF fibers were integrated with orthogonally arranged metal wires in a row-by-column configuration [19]. A fiber-like actuator was also reported in [31] where an extruded polyaniline fiber is coated with a thin layer of solid polymer electrolyte and an outer layer of polypyrrole acts as a counter electrode. Wang *et al* [32] has prepared a highly flexible polymer fiber battery by using polypyrrole composites. The research group of Wang [33] has developed a microfiber nanogenerator composed of a pair of entangled fibers which can generate electrical current using the piezoelectric effect. Solar energy is a clean, reliable and cost-efficient energy source. Studies on fiber-based flexible photovoltaic cells have been attracting considerable attention [34, 35]. A photovoltaic fiber design for smart textiles has been proposed [36], but its power conversion efficiency is still low. Finally, several groups [37–39] have recently demonstrated organic all-fiber transistors which can potentially allow the creation of electronic logic circuits by weaving.

Recently there have been several reports on capacitor fibers compatible with a textile weaving process. One possible application of a capacitor fiber is in distributed sensing of electrical influence, proximity, etc. By adding an external inductance such fibers make a resonant LC circuit, thus allowing the use of many highly sensitive resonant detection techniques which are able to detect small changes in the capacitor structure. Probably more interestingly, capacitor fibers together with energy harvesting fibers, promise an all-textile solution for the problem of wearable energy generation and storage, with the principal advantage of a capacitor over an electrochemical battery being a capacitor's almost unlimited cycle life. Among several proposals for a capacitor fiber we note a multicore fiber capacitor in the form of a bundle of $\sim$50 μm-sized coaxial cables connected in parallel on a micro-level (see [40]). However, such capacitors were never actually fabricated. Load bearing composite textiles comprising a large number of simple coaxial cables have been recently reported by the Air Force Research Laboratories [41] for distributed storage of electrical energy directly in the fuselage of an airplane for pulsed-weapon applications. This invention envisions reduction in the aircraft payload by combining mechanical and electrical functionalities in the same fiber. Finally, the group of Baughman [42] proposed carbon nanotube-based textile threads that can be adapted to build supercapacitor textiles after soaking such threads in an electrolyte.

In this paper we present a novel type of electronic fiber recently developed in our laboratory—high capacitance, soft fiber from conductive polymer composites. One key advantage of our fibers is that they do not require the use of electrolytes for their operation, which is especially desirable for wearable applications. Another key advantage is that the fibers can be made fully polymeric (no metallic electrodes) and very soft for applications in wearable sensing. Because of the relatively high capacitance of the fiber (60–100 nF m^{-1}) it can be also used for energy storage applications. In terms of capacitance our fibers take an intermediate position between the coaxial cables and supercapacitors. Thus, the capacitance of a coaxial cable with comparable parameters is typically 1000 times smaller than that of our fibers.

2. Fiber capacitor materials

The fiber capacitors presented in our paper are fabricated by the fiber drawing technique which consists of three steps. The first

step involves rolling or stacking conductive and dielectric films into a multilayer preform structure. During the second step the preform is consolidated by heating it to temperatures somewhat above the polymer glass transition temperature (T_g). Finally, the third step involved drawing of the consolidated preform into fibers using a fiber drawing tower. Drawing is typically performed at temperatures higher than the polymer T_g. During successful drawing the resultant fibers generally preserve the structured profile of a preform, thus fibers with very complex microstructure can be fabricated via homologous reduction (during drawing) of a macrostructure of the preform. The drawing technique used in this paper is directly analogous to the one used in the manufacturing of microstructured polymer optical fibers [43].

Flexible multilayer capacitors discussed in this paper generally consist of two conducting polymer layers serving as two electrodes of a capacitor, and two isolating polymer separator layers. To result in a successful drawing the preform materials should be compatible with each other in terms of their rheological and thermomechanical properties. In our first tests we have attempted the drawing of a thin continuous layer of low melting temperature metal sandwiched between two isolating polymer layers. As a metal we have used Bi58/Sn42 alloy with a melting point of 138 °C. Various polymers were tested as isolating layers. However, we found that in all cases it was difficult to preserve the laminated structure with a thin metal foil during the drawing process. In particular, when melted, metal foil would break into wires during drawing, thus destroying the continuous electrode structure. We have rationalized this observation by noting that the viscoelasticity, ductility and interfacial tension of alloy and the surrounding polymer cannot match well at drawing temperatures. For example, at the temperature for the polymer to be drawn into fibers the viscosity of the melted metal becomes very low. Thus it is easy for a thin sheet of melted metal to develop a flow instability and form several larger wires to minimize the surface energy associated with a polymer/metal interface. Another potential problem during drawing of metal sheets is that, when the polymer surrounding the molten metal becomes too soft, it can no longer hold the melt; as a consequence a large drop of metal would form at the preform end even before drawing starts, thus draining the rest of a preform from metal. From these initial experiments we have concluded that drawing of a thin metallic sheet sandwiched between two plastic sheets is, in general, problematic due to a strong mismatch of the material properties during the drawing process.

After realizing the challenge of drawing metallic electrodes in the form of thin sheets, a natural option to remedy this problem was to substitute metals with thermoplastic conductive polymers as electrodes. Unfortunately, thermoplastic intrinsic conductive polymers suitable for drawing are not available commercially. The only thermoplastic conductive polymers which are currently available commercially are either carbon-black-filled or, most recently, carbon-nanotube-filled films. In our research we have mostly used polyethylene(PE)-based carbon-black-filled films (BPQ series) provided by Bystat International Inc. The film, with a thickness of 91 μm, has a surface resistivity of 17 kΩ/sq. The measured volume resistivity is around 2.2 Ω m in the directions along the surface. To find the isolating materials that can be co-drawn with this conductive film, we have tried various polymer films such as polyvinylidene fluoride (PVDF), polycarbonate (PC), polyethylene terephthalate (PET), polymethyl methacrylate (PMMA) and others. Among all the attempted polymers we have found that the two best materials for the isolating layer were low density polyethylene (LDPE) film or a polycarbonate film. The fibers were either drawn bare or they were encapsulated into an electrically isolating PMMA jacket.

Finally, to connect drawn fibers several approaches were attempted. In one implementation the fiber only contained conductive polymer layers and to interrogate such fibers one had to introduce external probes into the fiber structure. In the second implementation either a small-diameter copper wire was integrated into the fiber during drawing, or a tin alloy electrode was drawn directly during fiber fabrication, thus providing a convenient way to connect one of the two probes. In the third implementation, two small copper wires were integrated during drawing, thus providing a convenient way to attach both electrical probes.

3. Capacitor fiber designs

Three distinct fiber capacitor geometries were successfully explored. The first fiber type features cylindrical geometry with two plastic electrodes in the form of a spiraling multilayer (see figure 1(a)). The central part of a fiber was either left empty with the inner plastic electrode lining up the hollow core, or a metallic electrode was introduced into the hollow core during drawing, or the core was collapsed completely, thus forming a plastic central electrode. In all these fibers, the second electrode was wrapped around the fiber. The second fiber type (see figure 1(b)) is also of cylindrical multilayer geometry. However, it features two hollow cores lined with two plastic electrodes. The fiber is wrapped into an isolating material so there is no direct contact with the environment. During drawing two metallic electrodes were introduced into the fiber cores. Finally, the third fiber type features a square electrically isolating tube comprising a zigzagging stack of the plastic electrodes (see figure 1(c)) separated by a zigzagging dielectric layer. The metallic electrodes were integrated on the left and right sides of a tube for the ease of connection.

Fibers of the first and second types (figure 1(a)) were fabricated by co-rolling of the two conductive polymer films which were physically and electrically separated by the two isolating LDPE films. In the resultant fiber the inner conductive film forms one electrode inside the hollow fiber core, while another electrode is created by the other conductive film at the fiber surface. The preform was thermally consolidated at 105 °C. Consolidation has been done by heating the preform to a temperature above the glass transition temperature (T_g) of the materials and then preserving it at this temperature for one hour before cooling down to room temperature. The diffusion of the polymer molecules through interfaces of adjacent layers fuses them together, thus reducing the effect of a property mismatch of different materials in the drawing process. After that the preform was drawn in a drawing tower at temperatures

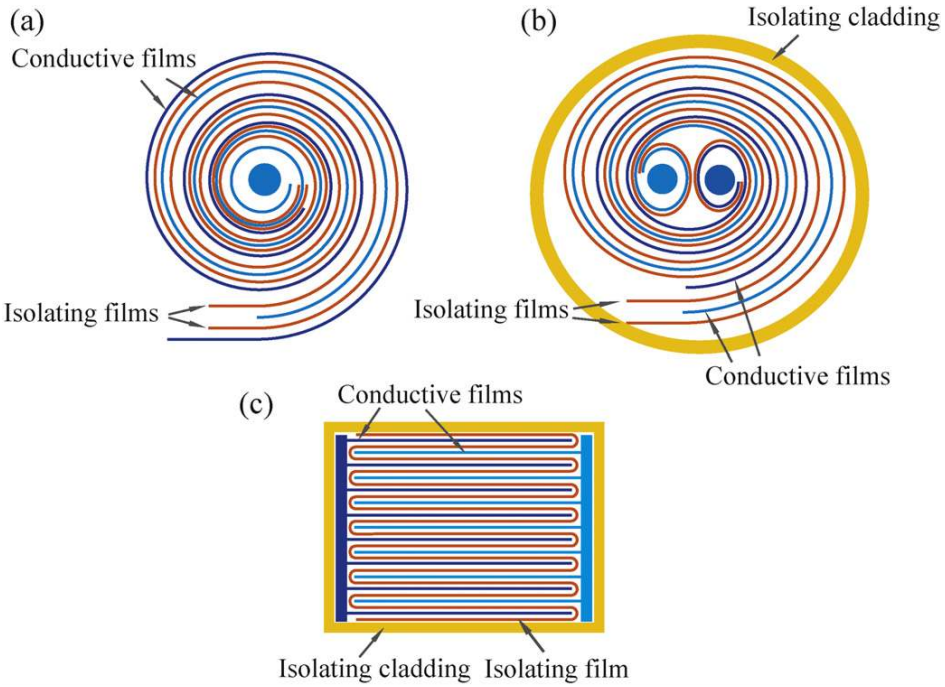

Figure 1. (a) Schematic of a cylindrical capacitor fiber preform featuring a spiraling multilayer comprising two conductive and two isolating films. The deep blue and light blue curves represent two conductive films, while red curves represent isolating LDPE films. (b) Schematic of a cylindrical capacitor fiber with two electrodes in the center. (c) Schematic of a rectangular preform prepared by encapsulating a zigzagging stack of two conductive and an isolating layer inside a rectangular PMMA tube. The deep blue and light blue curves represent conductive films, while the red curves represent isolating polycarbonate (PC) films.

in the range of 170–185 °C. A similar fabrication strategy was used in the fabrication of the second fiber type (figure 1(b)), with the only exception being positioning two isolated fiber cores in the fiber center, while encapsulating the fiber into an isolating HDPE plastic wrap. Finally, fibers of the third type (figure 1(c)) were created by encapsulating a zigzagging stack of electrodes and isolating layers inside a rectangular PMMA tube. After consolidation at 135 °C for one hour, the preform was drawn at temperatures around 200 °C.

4. Capacitor fiber connection and potential applications

An important issue when designing any smart fiber concerns connection of such fibers either to each other or with the external electrical probes. In view of various potential applications of a capacitor fiber we have explored several connection geometries. In figures 2(a)–(e) we show four complete designs for a capacitor fiber. In each figure we present both the structure of a preform before drawing, as well as the structure of a resultant fiber.

Design I is presented in figures 2(a) and (b) where we show a circular hollow core fiber with the first electrode formed by the conductive layer lining the hollow fiber core (see also figure 1(a)) and the second electrode formed by the other conductive layer wrapping the fiber from outside. The outside electrode is exposed for ease of access. The hollow core can be either collapsed (figure 2(b)) or left open during drawing (figure 2(a)). In general, to access the electrode inside the fiber core one has to use a needle-like electrical probe; in fact, we have used 50–100 μm diameter hypodermic needles to perform electrical characterization of this fiber. One of the advantages of the hollow core fibers is that they are very soft due to the lack of metallic components in their structure and, therefore, are most suitable for the integration into wearable textiles. Moreover, the hollow fiber core can be filled with functional liquids which will be in direct contact with one of the electrodes. This can be useful for various sensing applications, where physical or chemical properties of a liquid could be interrogated electrically.

Design II is presented in figure 2(c) where we show a circular hollow core fiber with one of the electrodes formed by a small 100 μm diameter copper wire which is integrated into the fiber core directly during drawing. With a tension-adjustable reel installed on the top of a preform, copper wire can be passed through the preform core, pulled down and embedded into the fiber center during drawing by collapsing the plastic cladding around it. The second electrode is formed by the other conductive layer wrapping the fiber from outside, similar to the first design. The main advantage of this design is the ease of connection to the inner electrode as the plastic capacitor multilayer can be easily stripped from the copper wire. This fiber has a lower effective resistivity compared to the hollow core fiber as one of the electrodes is made of a highly conductive metal. Despite the copper electrode in its structure the fiber is still highly flexible. As the outside of the

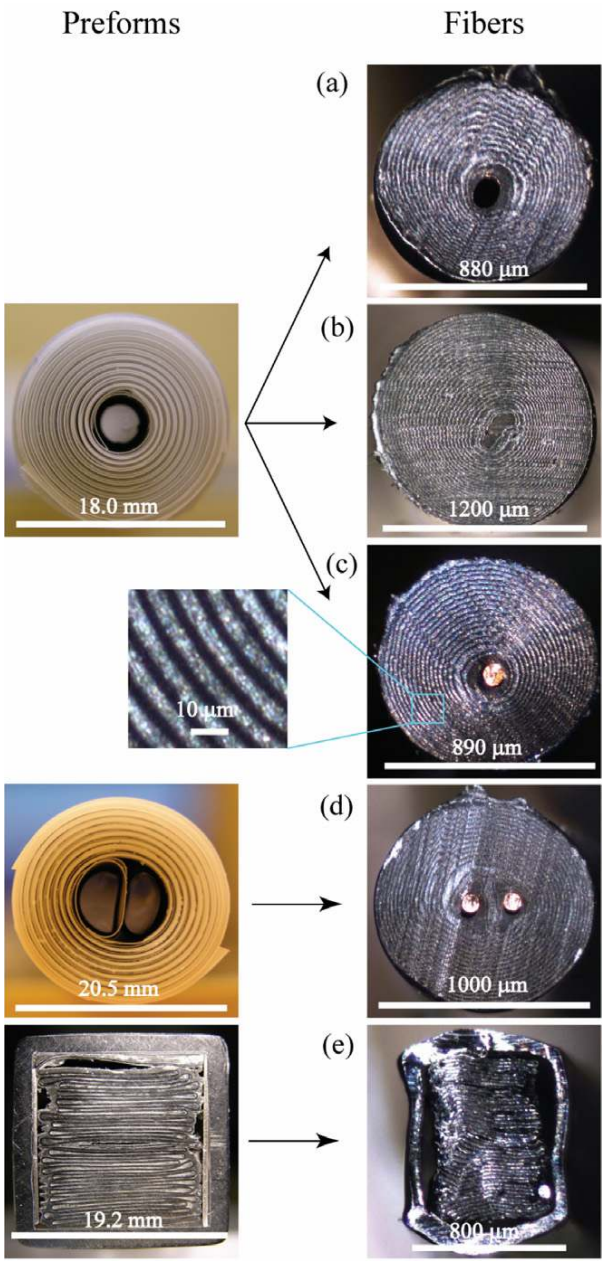

Figure 2. Design I: hollow core fiber with the first electrode lining the inside of a hollow core and the second plastic electrode wrapping the fiber from outside. During drawing the fiber hollow core can be left open (a) or collapsed (b) depending on the application requirement. Design II: hollow core fiber can be drawn with a metallic electrode in the center. Such an electrode can be a copper wire (c) in contact with the plastic electrode lining the hollow core. Design III: fiber containing two hollow cores. The cores are lined with two plastic electrodes electrically separated from each other. Fiber is drawn with two copper wires threaded through the hollow cores in the preform (d). Design IV: square fiber capacitor. Fiber features a zigzagging stack of two plastic electrodes separated by an electrically isolating PC layer (e). Furthermore, two metallic electrodes are placed in contact with plastic electrodes and the whole multilayer is encapsulated inside a square PMMA tube.

electrode is exposed, this fiber can be used for the detection of electromagnetic influence or as a proximity sensor.

Design III is presented in figure 2(d), where we show a circular fiber containing two hollow cores positioned in the middle of the fiber. Each core is lined with a distinct conductive layer which are forming electrodes 1 and 2. The cores with electrodes are electrically isolated from each other. Moreover, the whole preform is then wrapped in several layers of pure LDPE plastic to isolate the capacitor layers from the environment. The preform is then drawn with two copper wires threaded through its holes. The resultant fiber features two copper electrodes and a fully encapsulated capacitor multilayer. Such fibers can be interesting for energy storage applications due to ease of connection and electrical isolation from the environment.

Finally, design IV is presented in figure 2(e) where we show a thin PMMA tube of square cross section comprising a zigzagging multilayer of two conductive layers separated by a single electrically isolating PC layer. The first plastic electrode is located to the left and the second plastic electrode is located to the right of the isolating PC layer. At the left and right inner sides of the square tube we place foils of Bi58/Sn42 alloy in contact with the plastic conductive layers. During fiber drawing wire-like metallic electrodes are created from the foils. Finally, the structure of the resultant fiber is similar to the one of an encapsulated fiber with two copper electrodes.

In comparison with standard capacitors, we notice that a 10 nF ceramic capacitor in an 0210 package measures about 600 μm $\times$ 300 μm and 10 μF 0805 components measure 2.0 mm $\times$ 1.25 mm. The fiber capacitor does not possess advantages over the standard capacitors in terms of size, but the flexibility and softness it features are essential for applications in wearable smart textiles. On the other hand, encapsulating RC series in a single fiber makes the circuit in wearable e-textiles more compact and reliable because it may reduce the number of connection joints. Although the equivalent resistance of the capacitor is very high for a short fiber, which is limited by the properties of available conductive films, it can be reduced simply by increasing the length of the fiber as demonstrated in the following paragraphs. Moreover, the high resistance of the conductive film provides the fiber with a distributive nature, thus making it potentially applicable in touch-sensing of electrical influences, for example from a human finger.

5. Measurement of electrical characterization of capacitor fibers

To characterize electrical properties of our capacitor fibers we used a measurement circuit presented in figure 3, where the fiber capacitor is connected to a function generator (GFG-8216A, Good Will Instrument Co., Ltd) through the reference resistor $R_{\mathrm{ref}} = 480$ kΩ. The function generator provides a sinusoidal signal of tunable frequency $\omega = [0.3$ Hz–3 MHz]. An oscilloscope (GDS-1022, Good Will Instrument Co., Ltd) measures the input voltage $V_{\mathrm{Ch1}}(\omega)$ on channel 1 and the output voltage over the reference resistor $V_{\mathrm{Ch2}}(\omega)$ on channel 2. A 10X probe (GTP-060A-4, Good Will Instrument Co., Ltd) was

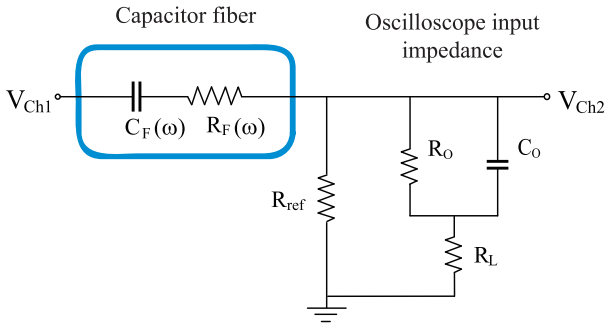

Figure 3. Diagram of the circuit model of the measurement set-up.

used to acquire the experimental data. The voltage produced by the function generator is fixed and in the whole frequency range of interest equals $V_{\mathrm{Ch1}} = 2$ V. In our experiments we measured both the amplitudes and the phase differences between channels 1 and 2. Due to the high resistivity of our fibers and also to fit the experimental data at higher frequencies ($\omega > 1$ kHz), we have to take into account the effective impedances of an oscilloscope.

To characterize capacitor fiber properties, we assume that they can be represented by an ideal capacitor with capacitance $C_{\mathrm{F}}(\omega)$ connected in series to an equivalent resistor with resistance $R_{\mathrm{F}}(\omega)$. This assumption is strictly valid when the fiber is uniform and when the two electrodes implanted into or wrapped around the capacitance fiber are of low resistance (meaning that there is no voltage differential along the fiber length). The detailed model for $C_{\mathrm{F}}(\omega)$ and $R_{\mathrm{F}}(\omega)$ of the fiber is developed in section 6.2. This model suggests that, at lower frequencies, these values are frequency-independent. The circuit model shown in figure 3 leads to

$$\frac{V_{\mathrm{Ch2}}}{V_{\mathrm{Ch1}}} = \{R_{\mathrm{ref}}[R_{\mathrm{O}} + R_{\mathrm{L}}(1 + \mathrm{j}\omega C_{\mathrm{O}} R_{\mathrm{O}})]\} \times \left\{ R_{\mathrm{ref}}[R_{\mathrm{O}} + R_{\mathrm{L}}(1 + \mathrm{j}\omega C_{\mathrm{O}} R_{\mathrm{O}})] + \left(R_{\mathrm{F}} + \frac{1}{\mathrm{j}\omega C_{\mathrm{F}}}\right) \times [R_{\mathrm{O}} + (R_{\mathrm{L}} + R_{\mathrm{ref}})(1 + \mathrm{j}\omega C_{\mathrm{O}} R_{\mathrm{O}})] \right\}^{-1}. \quad (1)$$

Before analyzing our capacitor fibers we perform a calibration measurement to find the effective circuit parameters, i.e. R_{O}, C_{O} and R_{L} of an oscilloscope. The calibration circuit is identical to that shown in figure 3 with the only exception being that, instead of a fiber, we use a known resistor $R_{\mathrm{F}} = 477$ kΩ and no capacitance C_{F}. Now we use the developed effective circuit model to characterize fiber capacitors. As an example, in figure 4 we present the electrical response of a 650 μm diameter, 137 mm long capacitor fiber. In figure 4(a) we present the ratio of amplitude ($|V_{\mathrm{Ch2}}/V_{\mathrm{Ch1}}|$) as a function of frequency and in figure 4(b) we present the phase difference (θ) between two channels also as a function of frequency. The measurements were taken in a small frequency region of $\omega \sim 1$ Hz–1 kHz and the fitting of datasets gives frequency-independent values of $C_{\mathrm{F}} = 9.8$ nF and $R_{\mathrm{F}} = 26$ kΩ.

6. Electrical properties of capacitor fibers

In this section we present the properties of fiber capacitance and resistance as a function of various fiber geometrical parameters. Most of the measurements presented in this section were performed on fibers featuring a single copper electrode in their cores, while the second electrode is formed by the plastic conductive layer on the fiber surface (see figure 2(c)). The fiber was co-drawn with a 100 μm thick copper wire in its center. In the preform, both conductive layers are 75 μm thick, while the two insulating layers are made of 86 μm thick LDPE films. Examples of drawn fibers of ∼1 mm diameter are presented in figure 5(a). To characterize capacitance fibers we used the embedded copper wire as the first electrical probe, while the second electrical probe was made by wrapping aluminum foil around a part or the whole of the fiber as shown in figure 5(b).

6.1. Effect of the shape of an electrical probe connected to the fiber outer electrode

To connect the capacitor fibers to a measurement circuit one has to use two electrical probes. One of the probes is naturally a copper wire going through the fiber center. The other probe has to be attached to the surface of the fiber outer plastic electrode. This electrode is quite resistive as it is made of a conductive plastic. Therefore, measured results will be strongly influenced by the geometry of the second probe. If a point probe is used to connect to the fiber outer electrode the measured resistance will be the highest, while if a distributed probe is used then the resistivity will be the smallest. This is easy to rationalize by noting that generally there will be two types of currents flowing through the fiber. The first current is transverse to the fiber direction, while the second one is along the length of the fiber. For the transverse current, resistivity of a fiber will be

$$R^{\mathrm{t}} \approx \rho_v \frac{S}{L d_{\mathrm{c}}}, \quad (2)$$

where ρ_v is the volume resistivity of the conductive films, L is the length of the fiber, S and d_{c} are respectively the width and thickness of the conductive films. For the longitudinal currents, fiber resistivity will be

$$R^{\mathrm{l}} \approx \rho_v \frac{L}{S d_{\mathrm{c}}}, \quad (3)$$

which for longer samples ($L > S$) is much higher than the resistivity for transverse currents. Clearly, when connecting to a fiber using a point probe, fiber resistivity will be dominated by its longitudinal component (3). On the other hand, when covering the fiber outer electrode with a continuous probe (such as metal foil shown in figure 4(b)) the effective fiber resistivity will be mostly determined by its transverse component given by equation (2), where L would be the probe length. As predicted by equation (2), in the case of a continuous probe, measured resistivity has to decrease for higher coverage ratios. We would like to note that an alternative and a more practical way of implementing a

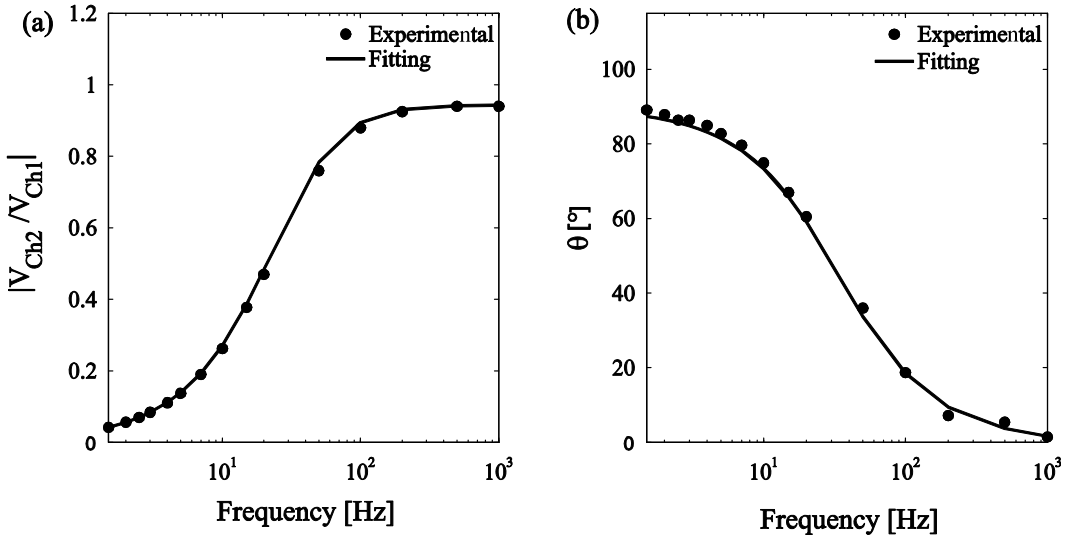

Figure 4. Example of fitting of the capacitor fiber parameters. Measured fiber is 650 μm in diameter and 137 mm in length. (a) and (b) represent the voltage drop and phase shift, respectively, versus frequency. Experimental data is shown as dots, while solid curves present a response of the effective circuit model with the fitted parameters.

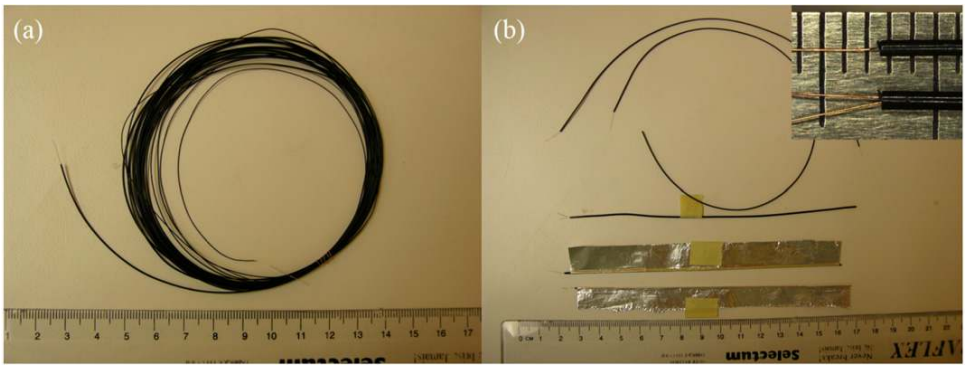

Figure 5. (a) Capacitor fiber fabricated from the preform shown in figure 2(c). The fiber features a central 100 μm thick copper wire, as well as an exposed conductive plastic electrode on the fiber surface. (b) To perform electrical characterization of the fibers, embedded copper wire is used as the first electrical probe, while the second electrical probe is an aluminum foil wrapped around the fiber conductive surface. The inset is an enlarged view of the fibers with single and double copper wire electrodes.

continuous low resistivity probe for the outside fiber electrode is to spray a highly conductive paint on the fiber surface.

Figure 6 demonstrates the effect of the outer electrode coverage ratio by a continuous probe on the fiber capacitance C_F and resistance R_F. The measured fiber was 780 μm in diameter and 202 mm in length containing 20 bilayers of conductive film. We can see that fiber resistance is indeed strongly affected by the electrode coverage ratio while the capacitance has a constant value around 13 nF. As seen from the figure, fiber resistance decreases from 440 to 120 kΩ as the electrode coverage ratio increases from 5% to 100%. As predicted by equation (2), measured resistivity decreases for higher electrode coverage ratios. However, this decrease is not purely inversely proportional to the coverage ratio due to the contribution of the longitudinal resistivity. Notably, capacitance of the fibers is not sensitive to the position and size of the electrodes. In these measurements the aluminum foil probe was always placed in the middle of the test fiber.

6.2. RC ladder network model for capacitor fibers fully covered with outer probes

The high resistivity of conductive composite films endows the capacitor fiber with a distributive nature. Thus its electrical behavior can be described better by a distributed network than a lumped RC circuit. In the condition that its outer electrode is fully covered with a highly conductive probe, the fiber can be described by an RC ladder circuit as shown in figure 7. Here, R^t is the transverse resistance of a single conductive film spiraling from the fiber core towards its surface with a distance of S. R^t is expressed by equation (2). C is the capacitance of the two co-rolled conductive films. As thicknesses of the

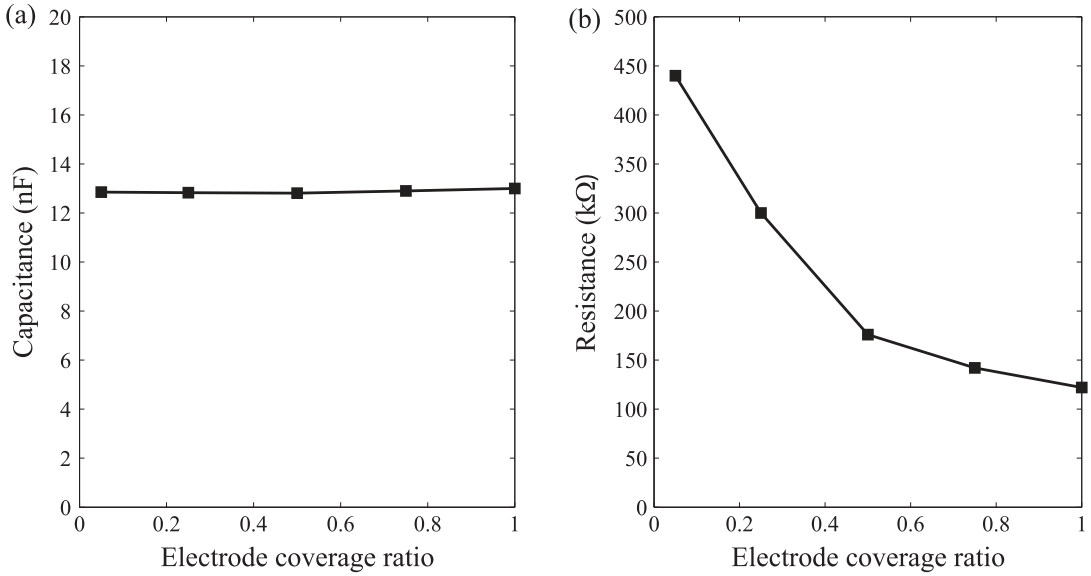

Figure 6. Effect of the electrode coverage ratio on the capacitance and resistance of a capacitor fiber with diameter of 780 μm and length of 202 mm.

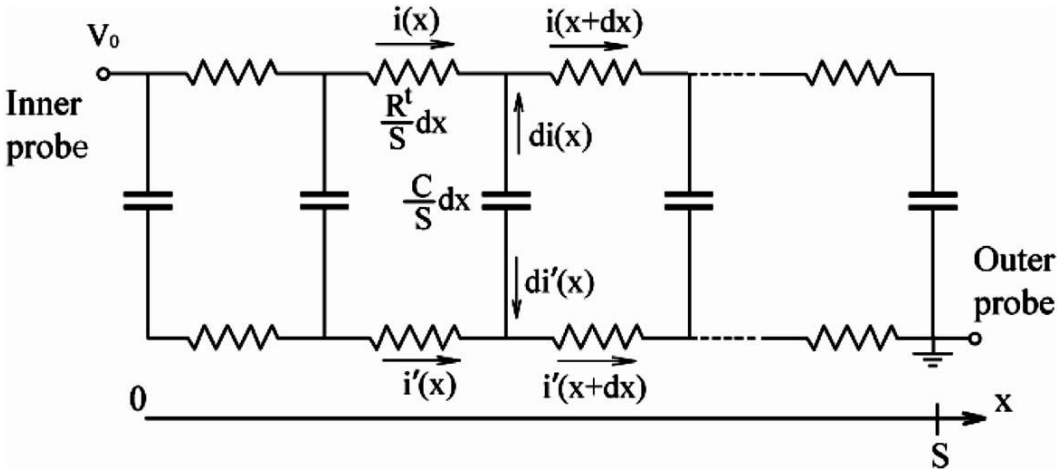

Figure 7. Ladder network model of the capacitor fiber fully covered with outer probe.

dielectric and conductive layers in the fiber are a hundred times smaller than the fiber diameter, fiber capacitance can be well approximated using an expression for the equivalent parallel-plate capacitor:

$$C \approx 2\varepsilon_0\varepsilon\frac{LS}{d_\mathrm{i}}, \tag{4}$$

where ε is the dielectric constant of the isolating films, ε_0 is permeability of the vacuum and d_i is the thickness of the rolled isolating films.

As shown in figure 7, $i(x)$ and $i'(x)$ denote the current flowing in the conductive film connected to the inner probe and outer probe, respectively. V_0 is the voltage difference between the inner probe and outer probe. We assume that the resistivity of the conductive film is a position-independent and frequency-independent parameter. Applying KVL and KCL to the ladder circuit leads to the following equations:

$$\int_0^x \frac{R^\mathrm{t}}{S} i(l)\,\mathrm{d}l + \frac{S}{\mathrm{j}\omega C}\frac{\mathrm{d}i'(x)}{\mathrm{d}x} + \int_x^S \frac{R^\mathrm{t}}{S} i'(l)\,\mathrm{d}l = V_0 \tag{5}$$

and

$$\mathrm{d}i(x) = -\mathrm{d}i'(x). \tag{6}$$

With boundary conditions

$$i(0) = i'(S) \qquad \text{and} \qquad i(S) = 0, \tag{7}$$

equations (5) and (6) can be solved analytically and yield the following expressions for the effective capacitance and effective series resistance:

$$C_\mathrm{F}(\omega) = -\frac{1}{\omega R\,\mathrm{Im}(f(B))} \tag{8}$$

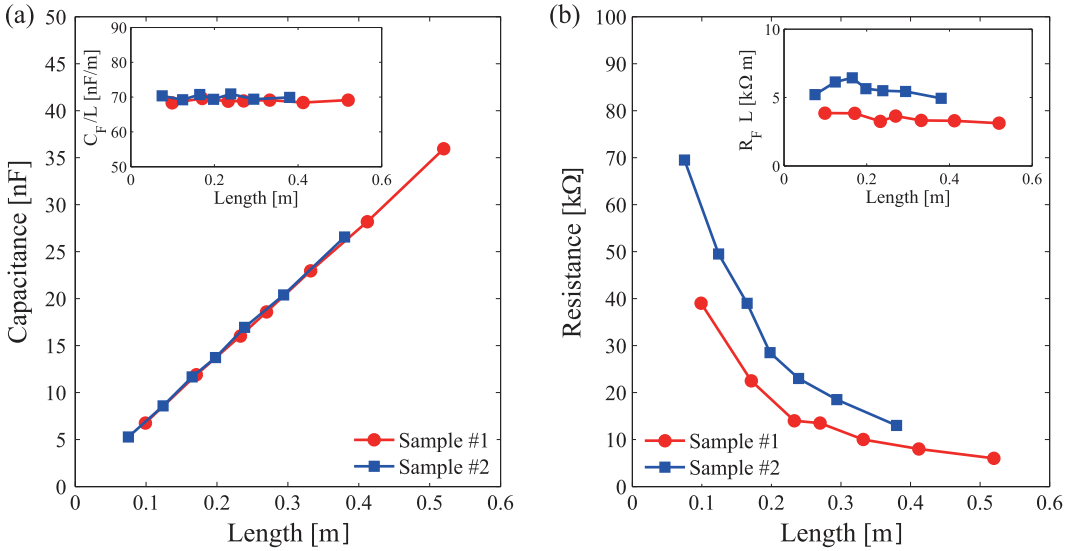

Figure 8. Dependence of the (a) fiber capacitance and (b) fiber resistivity on fiber length. Red and blue datasets correspond to the two fiber samples of different diameters drawn from the same preform. Insets: dependence of the (a) fiber capacitance per unit length C_F/L and (b) fiber resistivity factor $R_F L$ on the fiber length.

$$R_F(\omega) = \frac{R^t}{2} + R^t \,\mathrm{Re}(f(B)), \tag{9}$$

where

$$f(B) = \frac{1+\cosh(B)}{B\,\sinh(B)}; \qquad B = \sqrt{2j\omega R^t C}.$$

Note that at low frequencies, i.e. $B \to 0$, equations (8) and (9) reduce to the frequency-independent values as follows:

$$C_F = C, \qquad R_F = \tfrac{2}{3}R^t. \tag{10}$$

6.3. Effect of the capacitor fiber length

In order to study the dependence of the capacitor fiber properties as a function of fiber length, we have used two fiber samples that were drawn from the same preform. Sample #1 and sample #2 had outer diameters of 920–980 μm and 720–760 μm, respectively. Both samples were drawn from the same preform at speeds around 100 mm min^{-1} at 180°. The two samples were then cut into fiber pieces of different lengths ranging between 10 and 60 cm, and then wrapped with an aluminum foil with 100% coverage ratio. The experiments were conducted at low frequencies ($\omega < 1$ kHz). Thus effective capacitance and resistance can be expressed by constant values. In figure 8(a) we present measured fiber capacitance as a function of fiber length and observe a clear linear dependence. From this data we see that for all the fibers the capacitance per unit length is around 69 nF m^{-1} (inset of figure 8(a)), which is very close to the value of 69.5 nF m^{-1} measured for the capacitance of the fiber preform. This finding is easy to rationalize from equations (4) and (10). As S/d_i is constant during drawing (because of the largely homologous drawing), hence C_F/L should be the same for any fiber produced from the same preform, regardless of the fiber size. The reason why our fibers can obtain large capacitance is because the value of S/d_i is much larger than that of a coaxial cable with one capacitive layer. In contrast, fiber resistance decreases inversely proportional to the fiber length. In fact, it is rather the product $R_F L$ which is approximately constant, as shown in the inset of figure 8(b). Equations (2) and (10) indicate that, if ρ_v is constant, $R_F L$ should also be a constant because S/d_c is the same for fibers drawn from the same preform. However, we also find that the thinner fiber (sample #2) shows a larger value of $R_F L$. This diameter dependence is implied in the volume resistivity ρ_v in equation (2). It is reported that the resistivity of CB/polymer composites increase as the material is stretched, and the value is proportional to the elongation ratio in logarithm scale [44, 45]. Thus we observed that the thinner fiber has a larger $R_F L$ value.

6.4. Effect of the temperature of operation on the fiber electrical properties

The effect of the temperature of operation on the electrical properties of a capacitor fiber is presented in figure 9 for the example of two particular samples. Sample #1 was 135 mm long and had a diameter of 840 μm, while sample #2 was 133 mm long and had a diameter of 930 μm. To control the temperature of the two samples they were fixed to a hot plate. Our measurements at low frequencies show that fiber capacitance per unit length remains almost independent of the temperature of operation, while fiber resistivity increases as temperature rises. This result is in good correspondence with the recent reports on a positive temperature coefficient [46, 47] for the resistivity of the composites of carbon black and LDPE in the 0–100 °C temperature range. The effect of thermal expansion and a consequent increase of the average distance between carbon black particles are thought to be the main reasons for the positive temperature coefficient of such

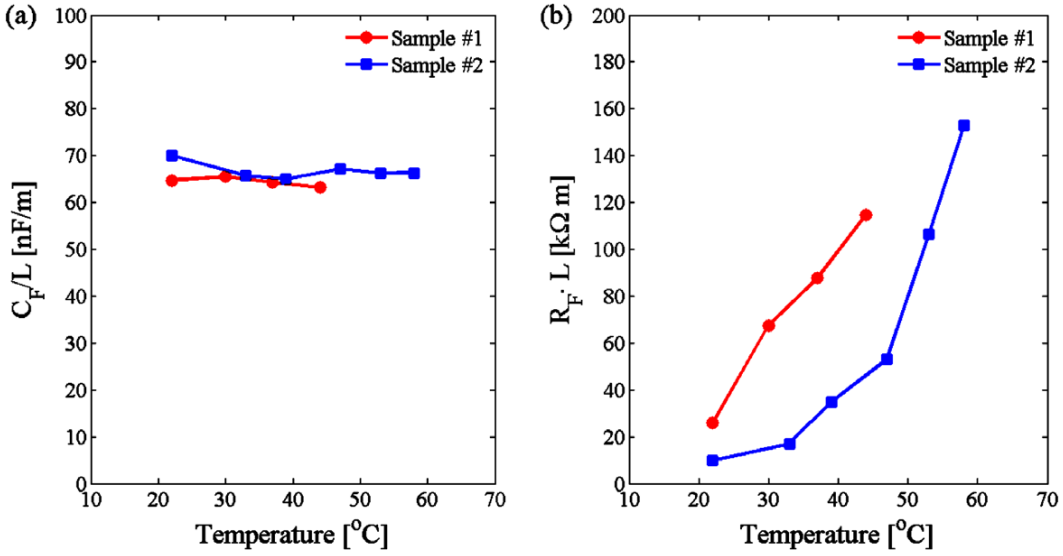

Figure 9. Effect of the temperature of operation on electrical properties of a capacitor fiber. (a) Capacitance per unit of length C_F/L. (b) Resistivity factor $R_F L$. Sample #1 has a diameter of 840 μm and a length of 135 μm. Sample #2 has a diameter of 930 μm and a length of 136 mm.

conductive polymer composites. This interesting property promises various applications of capacitor fibers in self-controlled or self-limiting textiles responsive to temperature or heat.

6.5. Frequency responses of the capacitor fiber

As predicted by equations (8) and (9) of the ladder network model, both the effective capacitance and effective resistance of a capacitor fiber should largely be dependent on frequency, while it can be approximated as constant in the low frequency region. In this section we will experimentally study the performance of the capacitor fiber as a function of frequencies. Besides the effect of the distributive nature of the fiber structure, there are two other factors that may contribute to the frequency dependence of the measured voltage over the reference resistor $V_{Ch2}(\omega)$. One is the impedance mismatch of the fiber and the measurement circuit, mainly the input impedance of the oscilloscope, which have been included in equation (1). Another is the frequency-dependent electrical property of the conductive film that our fibers were produced from. It has been reported [48] that near the percolation threshold the resistivity of CB/polymer films decreases with increasing frequency. In order to isolate these two effects from those of the fiber structure, which is modeled as the ladder circuit, we conducted measurements by the following procedure. We first measured the responses of a known resistor bearing a similar resistance as that of the fiber and determined that complex impedance of the measuring circuit (mainly an oscilloscope) becomes important only at frequencies higher than 100 kHz. We then studied frequency responses of the conductive film, and found that its resistivity is frequency-independent below 300 kHz. Thus we conclude that the measurement circuit and the property of the conductive film would not influence the fiber characterization if experiments are conducted under frequencies lower than 100 kHz. The frequency responses of a fiber capacitor with a diameter of 0.93 mm and length of 137 mm are displayed in figure 10. At low frequencies both C_F and R_F are constants but decrease when the frequency is higher than 1 kHz. This behavior is similar to that of a standard electrolytic capacitor and is well explained by the RC ladder network model with a characteristic response frequency of $1/R^tC \sim 4$ kHz. We can also see that equations (8) and (9) provide very good predictions of the experimental data by assuming $C = 9.4$ nF and $R^t = 25.5$ kΩ in the model.

6.6. Effect of the fiber drawing parameters

Electrical performance of the capacitor fibers is equally affected by the fiber geometrical parameters and by the fiber material parameters. In this section we show that fiber fabrication parameters such as fiber drawing temperature and fiber drawing speed can have a significant effect on the fiber resistivity, while also somewhat affecting the fiber capacitance. Generally, capacitor fibers presented in this paper can be drawn at temperatures in the range from 170 to 185 °C with drawing speeds ranging from 100 to 300 mm min^{-1}. Figure 11 presents capacitance per unit length C_F/L and fiber resistivity parameter $R_F L$ as functions of the fiber diameter at low frequencies. Several sets of data are presented for the fibers drawn from the same preform at various drawing temperatures and drawing speeds.

As seen from figure 11(a) fiber capacitance C_F/L is largely independent of the fiber diameter and drawing parameters, and equals that of the fiber preform. In contrast, the fiber resistivity parameter $R_F L$ is significantly affected by the drawing parameters. Although equations (2) and (10) predict that, similar to the fiber capacitance, the resistivity should not vary with fiber diameter, from figure 11(b) we

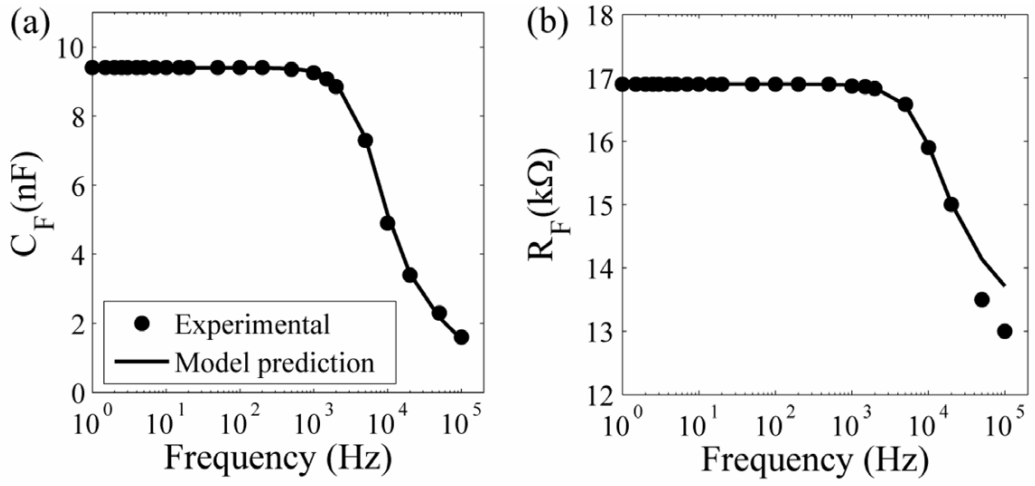

Figure 10. Comparison of experimental data and model predictions of frequency responses of a fiber capacitor. (a) Effective capacitance versus frequency. (b) Effective resistance versus frequency.

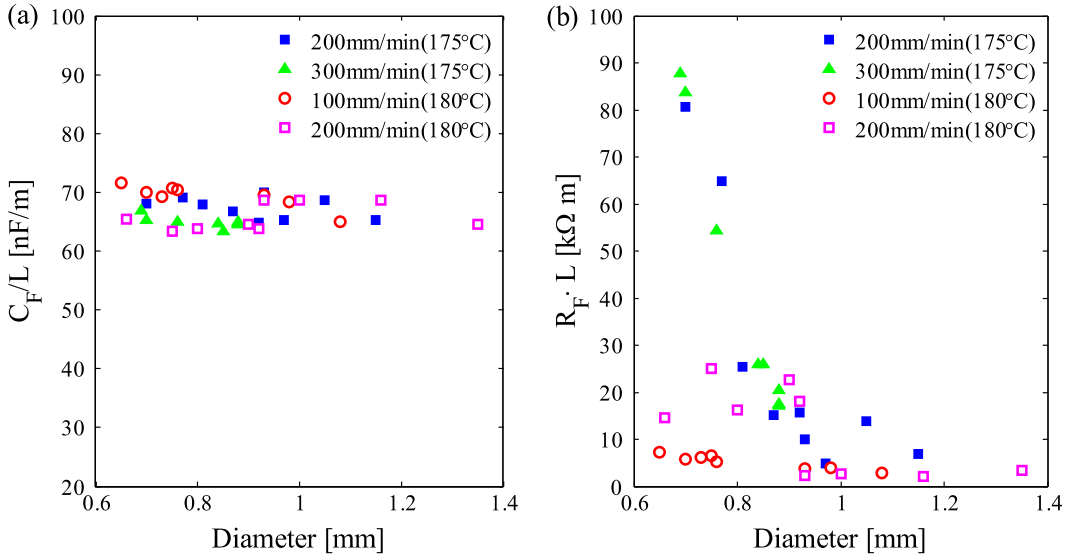

Figure 11. Electrical properties of the capacitor fibers as a function of fiber drawing parameters. (a) Capacitance per unit length C_F/L. (b) Resistivity parameter $R_F L$. Presented data is for fibers drawn at 175 and 180 °C with three different speeds of 100, 200 and 300 mm min^{-1}.

find that this statement is not true. With the same speed of 200 mm min^{-1}, fibers drawn at a temperature of 180 °C exhibit lower resistivity parameters than those drawn at 175 °C. At the same temperature of 180 °C, fibers drawn at a speed of 100 mm min^{-1} show lower resistivity parameters than those drawn at 200 mm min^{-1}. That is to say, fibers with the lowest resistivity are fabricated at higher temperatures and lower drawing speeds. It is in this regime that we could also produce the smallest diameter fibers. In particular, from equations (2), (4) and (10), fiber capacitance per unit length and the fiber resistivity parameter are related as

$$\frac{R_F L}{C_F/L} \propto \frac{\rho_v}{\varepsilon_0 \varepsilon}. \tag{11}$$

While fiber capacitance is indeed almost independent of the fiber geometrical and processing parameters, fiber resistivity is strongly influenced by them. This can be rationalized by concluding that bulk resistivity of the carbon black polymer composite can change significantly during the drawing procedure from its value in the preform. To further validate our observation that drawing at lower temperatures results in higher resistivities we performed a set of stretching experiments at room temperature on the planar conductive films. It was found that the resistivity of the conductive film increases as much as by two orders of magnitude from its original value when the films were stretched unheated to about two times their length. A similar observation has been reported

in the literature for carbon-black-filled polymers and polymer composites [44, 45].

The conclusions of these experiments can be rationalized as follows. During the drawing process the conductive polymer composite in the preform undergoes stages including heating, melting, stretching, annealing and cooling. The stretching increases the distance between the individual carbon black (CB) particles in the stretching direction, thus destroying the conductive network. During the annealing above the glass transition temperature, carbon black particles aggregate together through Brownian motion and form a continuous network. The destruction and reconstruction of conductive networks are highly dependent on the concentration and properties of CB and processing parameters such as mixing strength, temperature and time, and the annealing temperature and time, etc [49, 50]. If the fiber is drawn at a lower temperature and with a higher speed, the stronger viscous stress of the polymer matrix may disintegrate CB particles and reduce their aspect ratio, thus making the conductive network more difficult to be formed. The annealing conditions have a direct influence on the formation of the conductive network [50]. The increase of the annealing temperature decreases the viscosity of the matrix polymer, thus facilitating the movement and aggregation of CB particles. This in turn reduces the time needed for the CB particles to build up a conductive network. It is well reported that the resistivity of polymer composites filled with carbon black [50, 51] or carbon nanotubes [52] decreases as the annealing temperature and time increase. This explains our experimental observation about lower drawing speeds resulting in lower fiber resistivities, because a lower drawing speed leads to a longer annealing time in the furnace. In addition, a lower drawing speed corresponds to a weaker stretching and slower deformation. This not only avoids CB particles to be disintegrated but also provides them with more time to create a conductive network before cooling down to room temperature.

7. Conclusion

In this paper we present novel soft capacitor fibers made of conductive plastics and featuring a relatively high capacitance which is 3–4 orders of magnitude higher than that of a coaxial cable of comparable diameter. The fibers were fabricated using the fiber drawing technique which can be easily scaled up for industrial production. Fibers of various diameters from 650 μm to several mm have been demonstrated with a typical capacitance per unit length of 69 nF m^{-1} and a typical resistivity parameter of 5 kΩ m. It was also demonstrated that, during drawing, one or two metallic wire electrodes could be integrated into the fiber structure for ease of further connection. The developed capacitor fibers are ideally suited for integration into textile products as they are soft, small diameter, lightweight and do not use liquid electrolytes. Our measurements show that the fiber capacitance is a very stable parameter independent of the fiber diameter, operational temperature and electrical probe structure. In contrast, fiber resistivity has a very strong positive temperature coefficient. It is sensitive to stretching and strongly dependent on the shape of an electrical probe. We have also demonstrated that, while fiber capacitance is proportional to the fiber length, fiber resistivity is inversely proportional to the fiber length (assuming full electrode coverage). Due to the high resistivity of conductive composite films the capacitor fiber behaves like an RC ladder circuit. At low frequencies both C_F and R_F are constants but they decrease at frequencies higher than a specific value. We envision the use of the thus-developed capacitor fibers for various applications in electronic and smart textiles, distributed sensing and energy storage.

Acknowledgments

This project is supported in part by the NSERC and The Canada Council for the Arts New Media Initiative Karma Chameleon project, as well as the Canada Research Chair program. We would also like to thank Professor J Berzowska from Concordia University for fruitful discussions.

References

[1] Park S, Gopalsamy C, Rajamanickam R and Jayaraman S 1999 The wearable motherboard: flexible information infrastructure or sensate liner for medical applications *Stud. Health Technol. Inform.* **62** 252–8

[2] Park S, Gopalsamy C and Jayaraman 1999 Fabric or garment with integrated flexible information infrastructure *WO Patent Specification* 9964657

[3] Post E R and Orth M 1997 Smart fabric, or washable computing *Proc. 1st Int. Symp. Wearable Computers* pp 167–8

[4] Paradiso R, Gemignani A, Scilingo E P and De Rossi D 2003 Knitted bioclothes for cardiopulmonary monitoring *Proc. 25th Annu. Int. Conf., IEEE-EMB, Engineering in Medicine and Biology Society* vol 4, pp 3720–3

[5] Marculescu D *et al* 2003 Electronic textiles: a platform for pervasive computing *Proc. IEEE* **91** 1991–2016

[6] Anton S R and Sodano H A 2007 A review of power harvesting using piezoelectric materials 2003–2006 *Smart Mater. Struct.* **16** R1-21

[7] Swallow L M, Luo J K, Siores E, Patel I and Dodds D 2008 A piezoelectric fibre composite based energy harvesting device for potential wearable applications *Smart Mater. Struct.* **17** 025017

[8] Vigo T L and Frost C M 1985 Temperature-adaptable fabrics *Text. Res. J.* **55** 737–43

[9] Zhang X X, Wang X C, Tao X M and Yick K L 2005 Energy storage polymer/MicroPCMs blended chips and thermo-regulated fibers *J. Mater. Sci.* **40** 3729–34

[10] Engin M, Demirel A, Engin E Z and Fedakar M 2005 Recent developments and trends in biomedical sensors *Measurement* **37** 173–88

[11] De Rossi D, Della Santa A and Mazzoldi A 1999 Dressware: wearable hardware *Mater. Sci. Eng.* C **7** 31–5

[12] Paradiso R, Loriga G and Taccini N 2005 A wearable health care system based on knitted integrated sensors *IEEE Trans. Inf. Technol. Biomed.* **9** 337–44

[13] Morris D *et al* 2008 Wearable sensors for monitoring sports performance and training *5th Int. Workshop on Wearable and Implantable Body Sensor Networks* pp 121–5

[14] Drean E, Schacher L, Bauer F and Adolphe D 2007 A smart sensor for induced stress measurement in automotive textiles *J. Tex. Instrum.* **98** 523–31

[15] Gauvreau B, Guo N, Schicker K, Stoeffler K, Boismenu F, Ajji A, Wingfield R, Dubois C and Skorobogatiy M 2008 Color-changing and color-tunable photonic bandgap fiber textiles *Opt. Express* **16** 15677–93

[16] Tao X 2001 *Smart Fibres, Fabrics and Clothing* (Cambridge: Woodhead)

[17] Lam Po Tang S and Stylios G K 2006 An overview of smart technologies for clothing design and engineering *Int. J. Cloth. Sci. Technol.* **18** 108–28

[18] Dias T, Hurley W, Monaragala R and Wijeyesiriwardana R 2008 Development of electrically active textiles *Adv. Sci. Technol.* **60** 74–84

[19] Carpi F and De Rossi D 2005 Electroactive polymer-based devices for e-textiles in biomedicine *IEEE Trans. Inf. Technol. Biomed.* **9** 295–318

[20] De Rossi D, Carpi F, Lorussi F, Mazzoldi A, Scilingo E P and Tognetti A 2002 Electroactive fabrics for distributed, conformable and interactive systems *IEEE Sensors Conf. (Orlando, FL)*

[21] Pushparaj V L, Shaijumon M M, Kumar A, Murugesan S, Ci L, Vajtai R, Linhardt R J, Nalamasu O and Ajayan P M 2007 Flexible energy storage devices based on nanocomposite paper *Proc. Natl Acad. Sci. USA* **10** 13574–7

[22] Hu L, Pasta M, La Mantia F, Cui L, Jeong S, Dawn Deshazer H, Choi J W, Han S M and Cui Y 2010 Stretchable, porous, and conductive energy textiles *Nano Lett.* **10** 708–14

[23] Suga T, Konishi H and Nishide H 2007 Photocrosslinked nitroxide polymer cathode-active materials for application in an organic-based paper battery *Chem. Commun.* 1730–2

[24] Bhattacharya R, de Kok M M and Zhou J 2009 Rechargeable electronic textile battery *Appl. Phys. Lett.* **95** 223305

[25] Kim D-H, Ahn J-H, Choi W M, Kim H-S, Kim T-H, Song J, Huang Y Y, Liu Z and Rogers J A 2008 Stretchable and foldable silicon integrated circuits *Science* **320** 507–11

[26] Karaguzel B, Merritt C R, Kang T, Wilson J M, Nagle H T, Grant E and Pourdeyhimi B 2009 Flexible, durable printed electrical circuits *J. Text. Instrum.* **100** 1–9

[27] Bowman D and Mattes B R 2005 Conductive fibre prepared from ultra-high molecular weight polyaniline for smart fabric and interactive textile applications *Synth. Met.* **154** 29–32

[28] Shim B S, Chen W, Doty C, Xu C and Kotov N A 2008 Smart electronic yarns and wearable fabrics for human biomonitoring made by carbon nanotube coating with polyelectrolytes *Nano Lett.* **8** 4151–7

[29] Wijesiriwardana R, Dias T and Mukhopadhyay S 2003 Resistive fiber-meshed transducers *Proc. IEEE Int. Symp. on Wearable Computing* pp 200–5

[30] Huang C-T, Shen C-L, Tang C-F and Chang S-H 2008 A wearable yarn-based piezo-resistive sensor *Sensors Actuators* A **141** 396–403

[31] Mazzoldi A, Degl'Innocenti C, Michelucci M and De Rossi D 1998 Actuative properties of polyaniline fibers under electrochemical stimulation *Mater. Sci. Eng.* C **6** 65–72

[32] Wang J, Too C O and Wallace G G 2005 A highly flexible polymer fibre battery *J. Power Sources* **150** 223–8

[33] Qin Y, Wang X and Wang Z L 2008 Microfibre-nanowire hybrid structure for energy scavenging *Nature* **451** 809–13

[34] Berson S, de Bettignies R, Bailly S and Guillerez S 2007 Poly(3-hexylthiophene) fibers for photovoltaic applications *Adv. Funct. Mater.* **17** 1377–84

[35] O'Connor B, Pipe K P and Shtein M 2008 Fiber based organic photovoltaic devices *Appl. Phys. Lett.* **92** 193306

[36] Bedeloglu A, Demir A, Bozkurt Y and Sariciftci N S 2010 A photovoltaic fiber design for smart textiles *Text. Res. J.* **80** 1065–74

[37] Lee J B and Subramanian V 2005 Weave patterned organic transistors on fiber for e-textiles *IEEE Trans. Electron Devices* **52** 269–75

[38] Bonfiglio A, De Rossi D, Kirstein T, Locher I R, Mameli F, Paradiso R and Vozzi G 2005 Organic field effect transistors for textile applications *IEEE Trans. Inf. Technol. Biomed.* **9** 319–24

[39] Hamedi M, Forchheimer R and Inganäs O 2007 Towards woven logic from organic electronic fibres *Nature Mater.* **6** 357–62

[40] Cheng L F and Hong Y P 2001 Multifiber ceramic capacitor *J. Mater. Sci., Mater. Electron.* **12** 187–91

[41] Baron W, Blair M and Fries-Carr S 2006 Airframe structure-integrated capacitor *US Patent Specification* 6981671

[42] Dalton A B, Collins S, Muñoz E, Razal J M, Ebron V H, Ferraris J P, Coleman J N, Kim B G and Baughman R H 2003 Super-tough carbon-nanotube fibres *Nature* **423** 703

[43] Gao Y, Guo N, Gauvreau B, Rajabian M, Skorobogata O, Pone E, Zabeida O, Martinu L, Dubois C and Skorobogatiy M 2006 Consecutive solvent evaporation and co-rolling techniques for polymer multilayer hollow fiber preform fabrication *J. Mater. Res.* **21** 2246–54

[44] Feng J and Chan C-M 2003 Effects of strain and temperature on the electrical properties of carbon black-filled alternating copolymer of ethylene-tetrafluoroethylene composites *Polym. Eng. Sci.* **43** 1064–70

[45] Schulte B, Tischer W, Waldenrath W and Kaloff H 1988 Stretched polycarbonate films filled with carbon black *US Patent Specification* 4791016

[46] Tang H, Chen X and Luo Y 1997 Studies on the PTC/NTC effect of carbon black filled low density polyethylene composites *Eur. Polym. J.* **33** 1383–6

[47] Yu G, Zhang M Q and Zeng H M 1998 Carbon-black-filled polyolefine as a positive temperature coefficient material: effect of composition, processing, and filler treatment *J. Appl. Polym. Sci.* **70** 559–66

[48] Nakamura S and Sawa G 1998 Percolation phenomena and electrical conduction mechanism of carbon black-polyethylene composites *Proc. Int. Symp. Electrical Insulating Materials* p P1-54

[49] Zhang W, Dehghani-Sanij A A and Blackburn R S 2007 Carbon based conductive polymer composites *J. Mater. Sci.* **42** 3408–18

[50] Wu G, Asai S, Zhang C, Miura T and Sumita M 2000 A delay of percolation time in carbon-black-filled conductive polymer composites *J. Appl. Phys.* **88** 1480–7

[51] Cao Q, Song Y, Liu Z and Zheng Q 2009 Influence of annealing on rheological and conductive behaviors of high-density polyethylene/carbon black composites *J. Mater. Sci.* **44** 4241–5

[52] Alig I, Skipa T, Lellinger D and Pötschke P 2008 Destruction and formation of a carbon nanotube network in polymer melts: rheology and conductivity spectroscopy *Polymer* **49** 3524–32